AIP Advances

RESEARCH ARTICLE | AUGUST 08 2023

Terahertz broadband near-perfect absorber with a single-layer coating on doped semiconductor

Fenghua Shi ; Yihang Chen ; Chi-Wah Leung

Check for updates

AIP Advances 13, 085309 (2023)
https://doi.org/10.1063/5.0153206

View Online
Export Citation
CrossMark

10 August 2023 06:08:03

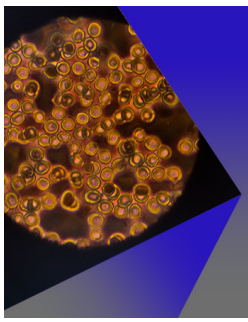

AIP Advances
Special Topic: Medical Applications of Nanoscience and Nanotechnology
Submit Today!
AIP Publishing

AIP Publishing

Terahertz broadband near-perfect absorber with a single-layer coating on doped semiconductor

Cite as: AIP Advances 13, 085309 (2023); doi: 10.1063/5.0153206
Submitted: 5 April 2023 • Accepted: 7 July 2023 •
Published Online: 8 August 2023

View Online Export Citation CrossMark

Fenghua Shi,[1,a)] Yihang Chen,[2] and Chi-Wah Leung[3,a)]

AFFILIATIONS

[1] Anhui Province Key Laboratory of Optoelectric Materials Science and Technology, School of Physics and Electronic Information, Anhui Normal University, Wuhu 241002, China
[2] Guangdong Provincial Key Laboratory of Quantum Engineering and Quantum Materials, School of Physics and Telecommunication Engineering, South China Normal University, Guangzhou 510006, China
[3] Department of Applied Physics, Hong Kong Polytechnic University, Hung Hom, Hong Kong

[a)] **Authors to whom correspondence should be addressed:** fhshi@ahnu.edu.cn and dennis.leung@polyu.edu.hk

ABSTRACT

We demonstrate that a single-layer coating on a doped GaAs or Si substrate enables broadband antireflection and, hence, broadband perfect absorption in the terahertz frequency range. This broadband behavior can be generally expected when the substrate material has a Drude-type dispersion. Our mathematical analyses show that the reflection from Drude-type material may have an anomalously dispersive phase shift. The anomalous dispersion of the reflection phase is used to compensate for the normal dispersion of the accumulation phase in the single-layer coating film. Consequently, the antireflection conditions are satisfied in a wide frequency range, and broadband antireflection is achieved. Thus, broadband perfect absorption is realized with only a single-layer coating film on the substrate. Our method provides a simple and efficient approach to achieving broadband perfect absorption, which is critical in many applications such as radar stealth techniques and solar cells.

© 2023 Author(s). All article content, except where otherwise noted, is licensed under a Creative Commons Attribution (CC BY) license (http://creativecommons.org/licenses/by/4.0/). https://doi.org/10.1063/5.0153206

10 August 2023 06:08:03

I. INTRODUCTION

Perfect absorption of incident electromagnetic (EM) waves is important for both fundamental studies and practical applications, such as light–matter interactions, thermal emitters, photodetectors, light modulators, and electromagnetic radiation camouflage.[1–6] Dielectric or magnetic loss absorbers were initially proposed at microwave frequencies.[7–9] Over the past ten years, metamaterial perfect absorbers (MPAs) have drawn extensive attention.[10–16] The typical configuration of MPAs usually consists of periodic metallic resonators at the top, a middle dielectric insulating layer, and a metallic ground plate. Most MPAs inherently operate within a narrow bandwidth due to the resonant nature of a single metamaterial unit cell. Dual- or multi-band absorption can be realized by combining multiple resonator units in an MPA. For example, MPAs composed of metallic resonators of different sizes arranged side-by-side at the top layer or stacked in the vertical direction enabled multi-band characteristics.[17–19] However, these multiband MPAs present two main drawbacks that greatly hamper their practical applications. One drawback is the complexity of fabricating and controlling these structures. Another disadvantage is the peak-dip-hump feature in the absorption spectrum, which makes these multiband MPAs unsuitable for broadband perfect absorption applications. Although the peak-dip-hump lineshapes can be alleviated by highly overlapping the discrete absorption bands in the spectrum, the achievable overall absorption bandwidth is limited due to the finite ability to increase the number of absorption peaks.

Broadband perfect absorption has always been one of the most important aspects for practical applications in various industrial and military fields.[20–22] It can better fulfill practical needs compared to most multi-band absorbers. Achieving broadband perfect absorption through multilayer antireflection coatings requires precise control of the complex process involving multiple depositions.[7,23] In

© Author(s) 2023

recent years, new methods have been explored to develop broadband perfect absorbers with simple structures.[24–28] For instance, Liu *et al.* (Ref. 24) proposed a broadband absorber with a periodic monolayered graphene patch array as the top layer, achieving continuous absorption of over 98% in the range of 1.2–1.7 THz. Huang *et al.* (Ref. 25) combined metallic circles and disks concentrically as the upper planner periodic resonator, resulting in a continuous absorption of over 99% in the broadband range of 9.06–9.8 THz. Huang *et al.* (Ref. 26) proposed a thin membrane silicon metasurface absorber with periodic elliptical holes, achieving continuous absorption of over 90% in the range of 1.1–1.6 THz. These simple-structured broadband absorbers not only enable easy fabrication and low cost but also allow highly efficient tunability of the absorption performance over broadband. In another work by Zheng *et al.* (Ref. 28), a VO_2 disk and a concentric square frame structure were used as the upper planner periodic resonator, resulting in a shift in absorption from 1% to 99% over the entire range of 4.2–6.5 THz. However, in these newly developed simple-structured broadband absorbers, lithography techniques are still required because they all involve a top metallic or dielectric periodic array. Semiconductor materials, which are significant in the terahertz regime, are seldom considered.

In this work, we propose a dispersion compensation strategy to achieve broadband perfect absorption with a single-layer coated semiconductor substrate. Dispersion compensation strategies have been adopted to achieve broadband responses in metamaterial designs.[29–31] Here, we propose a different dispersion compensation scheme based on the Drude dispersion of doped semiconductors. Simulation results demonstrate that a 300 μm-thick doped GaAs substrate coated with a 10 μm-thick polystyrene (PS) thin film achieves near-perfect absorption (99%) over a broad bandwidth (from 3.2 to 4.8 THz) at normal incidence. The absorber also maintains a relatively broad absorption bandwidth over a wide range of incident angles. Additionally, it is found that the position of the absorption band can be shifted by varying the doping concentration of the semiconductor substrate and the corresponding coating film thickness. Our proposed strategy can be applied to other material systems, such as absorbing materials with Lorentz responses at infrared frequencies[32] or damping elastic metamaterials.[33,34] The method we present offers a feasible and efficient approach to realizing broadband near-perfect absorption with a simple configuration and easy fabrication processes. This opens up possibilities for a wide range of terahertz functional devices with potential applications.

II. DESIGN PRINCIPLE AND MODEL CALCULATION

Consider that a single-layer coating is deposited on an absorbing substrate. The coating layer is assumed to have non-dispersive and non-absorptive optical properties. When the underlying absorbing medium is non-dispersive, the phases of reflection from the upper and lower interfaces of the coating film, denoted as $\phi(r)$ and $\phi(\rho)$, respectively, are also non-dispersive, as schematically shown in Fig. 1(a). In this case, the round-trip phase of the incident

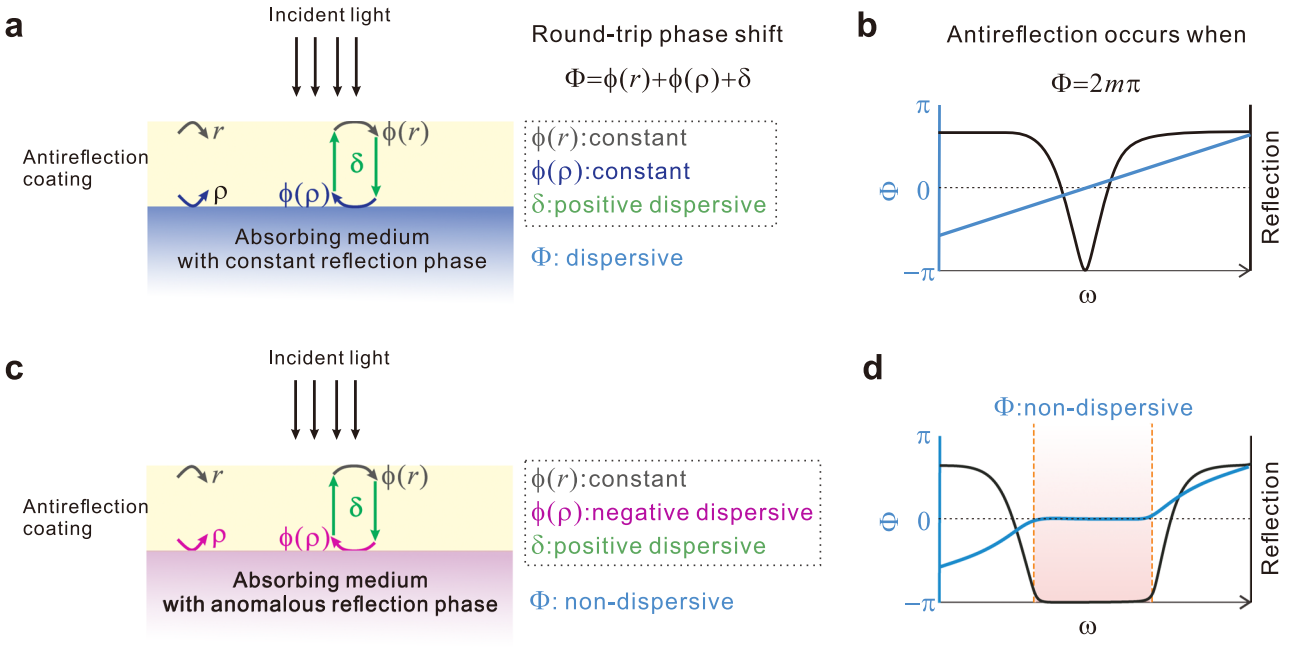

FIG. 1. Principle of a single-layer broadband antireflection coating for absorbing medium with an anomalous reflection phase. The round-trip phase Φ of light in the coating film is the sum of the reflection phases $\phi(r)$, $\phi(\rho)$, and the propagation phase δ. Generally, the phase change of light waves reflected from the coating/air interface $\phi(r)$ is a constant. (a) For normal absorbing material, the reflection phase upon the coating/absorbing-medium interface $\phi(\rho)$ is also a constant. The dispersion property of Φ is only determined by that of δ. (b) The typical narrowband antireflection occurs in the bilayered structure shown in (a). (c) For the absorbing material with negative dispersive $\phi(\rho)$, Φ can remain non-dispersive due to the dispersion compensation of $\phi(\rho)$ and δ. (d) The possible broadband antireflection by using the bilayered structure in (c).

10 August 2023 06:08:03

© Author(s) 2023

light in the coating film, denoted as Φ, is equal to the sum of the reflection phases $\phi(r)$ and $\phi(\rho)$, along with the propagation phase δ, i.e., $\Phi = \phi(r) + \phi(\rho) + \delta$. As a result, the frequency dispersion of Φ depends solely on the frequency dispersion of δ. The propagation phase δ is given by $\delta = 2dn_c\omega/c$, where d represents the thickness of the coating film and n_c is its refractive index. Here, ω denotes the angular frequency, and c represents the speed of light in a vacuum. It can be observed that δ increases with an increase in frequency, indicating that δ exhibits positive dispersion. Consequently, Φ also exhibits positive dispersion, as depicted in Fig. 1(b). Considering that antireflection occurs when $\Phi = 2m\pi$ (where m is an integer), one can anticipate that reflection dips will appear only at specific frequencies in the spectrum.

By contrast, let us consider another coating structure in which the reflection phase $\phi(\rho)$ at the interface between the coating film and absorbing substrate exhibits negative dispersion, as shown in Fig. 1(c). This anomalous reflection phase (normal reflection phase is either non-dispersive or positive dispersive) can be achieved when the refraction index of the substrate medium follows a Drude-type behavior near the resonant frequency,[35–38] as we will demonstrate in the subsequent discussions. Consequently, the positive dispersion of the propagation phase δ can be effectively compensated by the negative dispersion of $\phi(\rho)$ within a specific frequency range. As a result, the round-trip phase Φ remains almost unchanged over a broad bandwidth, as shown in Fig. 1(d). Moreover, the phase-matching condition $\Phi = 2m\pi$ might be simultaneously or nearly satisfied. Hence, one can expect that broadband antireflection can be achieved with a single-layer coating.

We now focus on the problem of determining the conditions under which a negative dispersive reflection phase $\phi(\rho)$ occurs. According to Fresnel's equations, the reflection coefficient from the interface between the coating and the absorbing substrate is defined as follows:[39]

$$\rho = \frac{n_c - n_s}{n_c + n_s}, \tag{1}$$

where n_c and n_s are the refraction indices of the coating film and the substrate, respectively. Taking into account the absorption in the substrate, the imaginary part of n_s is non-negligible. We set $n_s = n + jk$, where k is proportional to the absorption coefficient of the substrate. Substituting $n_s = n + jk$ into Eq. (1), we can obtain

$$\rho = \frac{n_c^2 - n^2 - k^2 - 2jn_ck}{(n_c + n)^2 + k^2}. \tag{2}$$

Hence, the reflection phase $\phi(\rho)$ can be derived as

$$\phi(\rho) = arctan\frac{2n_c}{\frac{n^2 - n_c^2}{k} + k}. \tag{3}$$

It can be seen from Eq. (3) that $\phi(\rho)$ may either increase or decrease with k, depending on the value of $k/\sqrt{n^2 - n_c^2}$. In the case

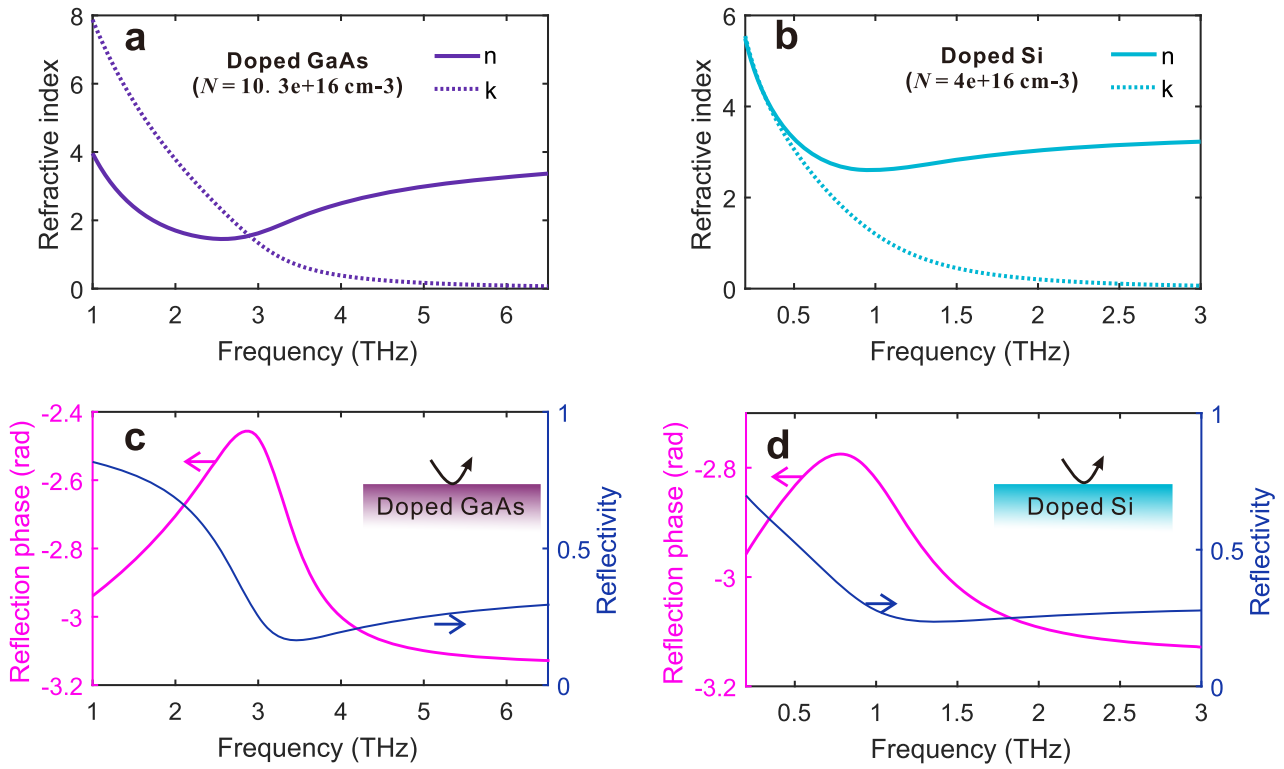

FIG. 2. Complex refractive indices of (a) doped GaAs and (b) doped Si substrates, respectively. These index spectra are calculated by Drude models with fitting parameters from Refs. 37 and 38. The reflection amplitudes and phases at (c) air/doped-GaAs and (d) air/doped-Si interfaces.

10 August 2023 06:08:03

© Author(s) 2023

of $0 < k/\sqrt{n^2 - n_c^2} < 1$, $\phi(\rho)$ increases as k increases. Conversely, if $k/\sqrt{n^2 - n_c^2} > 1$, $\phi(\rho)$ decreases as k increases. In the situation where $0 < k/\sqrt{n^2 - n_c^2} < 1$, both $\phi(\rho)$ and k exhibit the same tendency to change with frequency, i.e., dispersion. Consequently, When k displays negative dispersion, it can be expected that the reflection phase $\phi(\rho)$ will also exhibit negative dispersion.

For materials of the Drude type, it is possible to simultaneously satisfy the conditions of $0 < k/\sqrt{n^2 - n_c^2} < 1$ and have a negative dispersion of k at frequencies above the plasma frequency ω_p. This is because the material losses tend to decrease as the frequency exceeds ω_p). As a result, it becomes feasible to achieve a negatively dispersive reflection phase under these circumstances.

The Drude model is capable of accurately describing the optical properties of moderately and highly doped semiconductors, with their plasma frequencies typically falling within the terahertz spectral range. Figures 2(a) and 2(b) demonstrate the complex refractive indices of doped GaAs and Si, respectively, which have been calculated using Drude models fitted to experimental data obtained from previous studies.[37,38] The conductivity of the semiconductor, $\sigma(\omega)$, can be effectively represented using a Drude model,

$$\sigma(\omega) = \frac{Ne^2\tau}{m^*(1 - j\omega\tau)}, \tag{4}$$

where ω represents the angular frequency of the electromagnetic wave, N denotes the carrier concentration, τ is the scattering time, e is the elementary charge, and m^* is the effective carrier mass. The value of τ can be derived from the measured dc mobility by $\mu = e\tau/m^*$. The optimized values of N, m^*, and μ for GaAs and Si are obtained through a Drude fit to the THz transmission data as reported in Refs. 37 and 38. For n-type doped GaAs in Fig. 2(a), the values are $N = 10.3 \times 10^{16}$ cm^{-3}, $\mu = 4000$ cm^2 V^{-1} s^{-1}, and $m^* = 0.079m_0$ (where m_0 is the free electron mass). For n-type doped Si in Fig. 2(b), the values are $N = 4 \times 10^{16}$ cm^{-3}, $\mu = 1100$ cm^2 V^{-1} s^{-1}, and $m^* = 0.26m_0$. Subsequently, the dielectric constant $\varepsilon(\omega)$ can be obtained from $\sigma(\omega)$ using the equation,

$$\varepsilon(\omega) = \varepsilon_d - \frac{j\sigma(\omega)}{\omega\varepsilon_0}, \tag{5}$$

where ε_d denotes the dielectric constant of the undoped semiconductor.

III. RESULTS AND DISCUSSION

A single layer of PS coating is applied to a doped GaAs substrate for broadband antireflection, as shown in Fig. 3(a). The substrate has a thickness of 300 μm to prevent the transmission of terahertz waves. The transfer matrix method (TMM),[40] an analytical method commonly used to study simple and homogeneous models, is conventionally employed to calculate the reflectivity spectra of our structure. Figure 3(b) illustrates the reflection spectra of the Doped GaAs substrate with and without coating. It is evident that the reflection is significantly reduced by applying a single layer of coating. Particularly, near-complete antireflection and near-perfect absorption are maintained over a broad frequency range.

We now focus on the frequency range of 3.2–4.7 THz, where broadband near-complete antireflection occurs. Near-complete antireflection is achieved under two conditions: (i) $|r| \approx |\rho|$ and (ii) $\Phi = \phi(r) + \phi(\rho) + \delta = 2m\pi$. To satisfy condition (i), a dielectric coating material with a refractive index of 1.6, such as PS, is selected.[41–43] This ensures that the magnitudes of the reflection coefficients $|r|$ and $|\rho|$ are roughly equal in the desired frequency range, as shown in Fig. 3(c). In Fig. 3(d), it can be observed that with a 10 μm-thick PS coating, Φ (dark dashed line) is close to zero, indicating an approximate satisfaction of condition (ii) across the 3–5 THz range. This achievement is significant considering that traditional single-layer antireflection coatings can only satisfy condition (ii) at specific frequencies. Such a broadband feasibility of condition (ii) is attributed to the dispersion compensation of δ and $\phi(\rho)$. It is noteworthy that within the 3–5 THz frequency range, δ exhibits similar values to $\phi(\rho)$ but with opposite signs, and their compensation leads to the successive fulfillment of condition (ii).

In the design of a broadband single coating for doped GaAs substrates, it is necessary to carefully calculate the refractive index and thickness of the coating film to satisfy conditions (i) and (ii) separately. For condition (i), the refractive index of the coating film should be chosen to match the refractive indices of air and the substrate, ensuring excellent antireflection characteristics. At the same time, the antireflection coating is desired to operate over a broad frequency range. We observe that the amplitude spectrum of reflection from the coated/doped GaAs interface, denoted as $|\rho|$ [see Fig. 3(c)], exhibits a gentle dip at 3.7 THz, indicating the possibility of a rough index match in that vicinity. As shown in Fig. 3(c), the amplitude spectrum line of reflection from air/PS, denoted as $|r|$, crosses the gentle dip of the $|\rho|$ spectrum. This leads to a broadband approximate satisfaction of condition (i) from 3.2 to 4.9 THz. Regarding condition (ii), the thickness of the coating film determines the dispersion slope and values of δ, which in turn affect the degree of dispersion compensation with $\phi(\rho)$ and the final values of Φ. In our design shown in Fig. 3, the PS coating is set at 10 μm thick, ensuring that the absolute values of $\phi(\rho)$ and δ are similar but with opposite signs at frequencies from 3.2 to 4.8 THz. Consequently, the round-trip phase of Φ remains close to zero throughout the corresponding frequency range.

Due to the nontrivial reflection phase[44] (not equal to 0 or π) at the interface between the coating film and the semiconductor substrate in the structure shown in Fig. 3, the thickness of the coating film (10 μm) is 47% less than that of a quarter-wave plate at 4 THz (18.75 μm). The reduced film thickness contributes to the robust optical properties of the antireflection coating with respect to the angle of incidence. To demonstrate this, we calculate the absorptivity for both s- and p-polarized incidence waves at an angle of incidence of $\theta = 15°$, $30°$, $45°$, $60°$, and $75°$ [Figs. 4(a) and 4(b)]. The results show that the absorption feature remains prominent for incidence angles ranging from $0°$ to $60°$. Even at a high incidence angle of $60°$, the absorption remains above 90% within the considered frequency range for both polarizations.

Furthermore, the operating frequency band of broadband antireflection in such an optimized bilayered structure can be tuned by changing the carrier concentration of the doped GaAs and the corresponding thickness of the coating film, as shown in Fig. 5. The plasma frequencies and, therefore, the optical properties of

10 August 2023 06:08:03

© Author(s) 2023

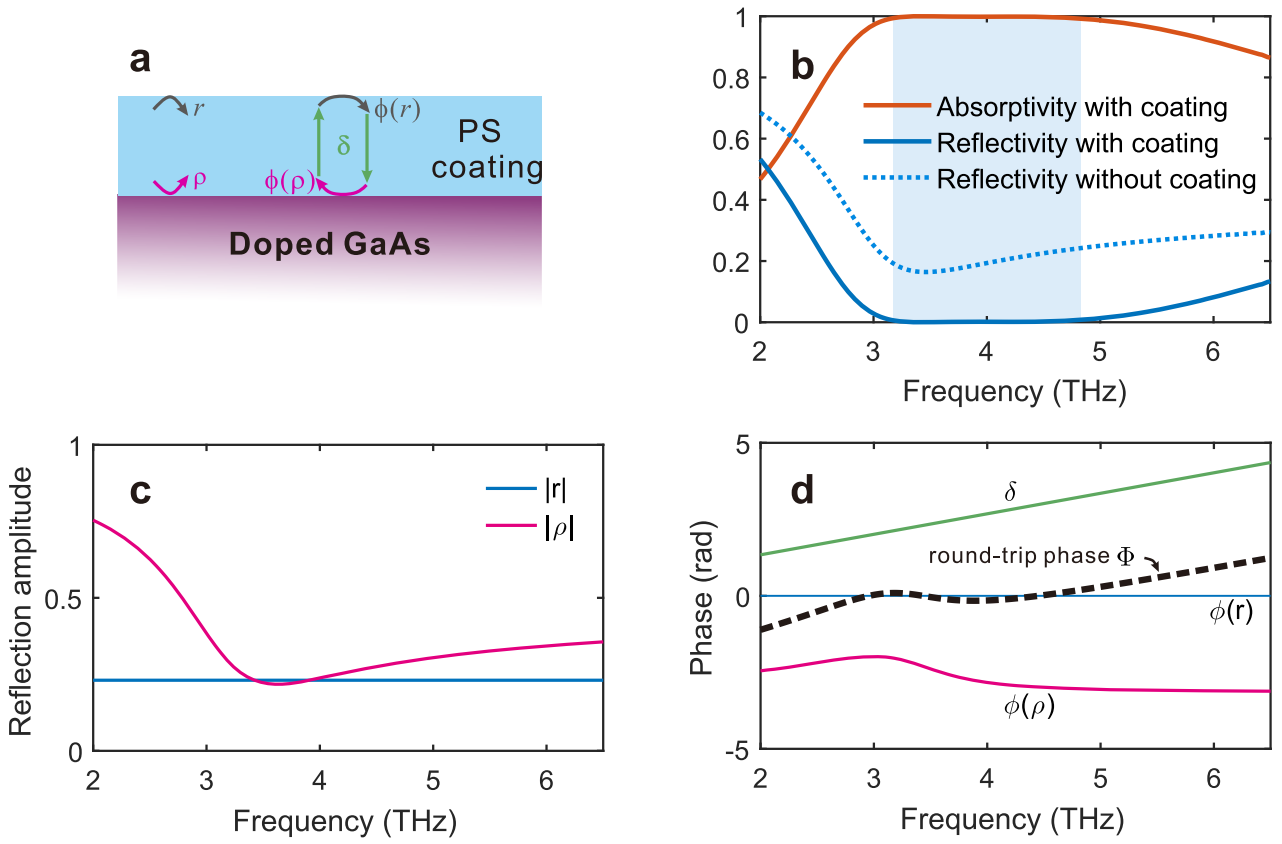

FIG. 3. (a) Schema of the PS-coated doped GaAs substrate. Here, the PS coating is 10 μm thick, and the carrier concentration of the *n*-type doped GaAs is $N = 10.3 \times 10^{16}$ cm^{-3}. (b) Absorptivity and reflectivity spectra of the doped GaAs with the PS coating layer, as well as the reflectivity spectra of the doped GaAs without the PS coating. (c) The spectra of reflection amplitudes $|r|$ and $|\rho|$. (d) The dispersion properties of phases $\phi(r)$, $\phi(\rho)$, σ, and Φ.

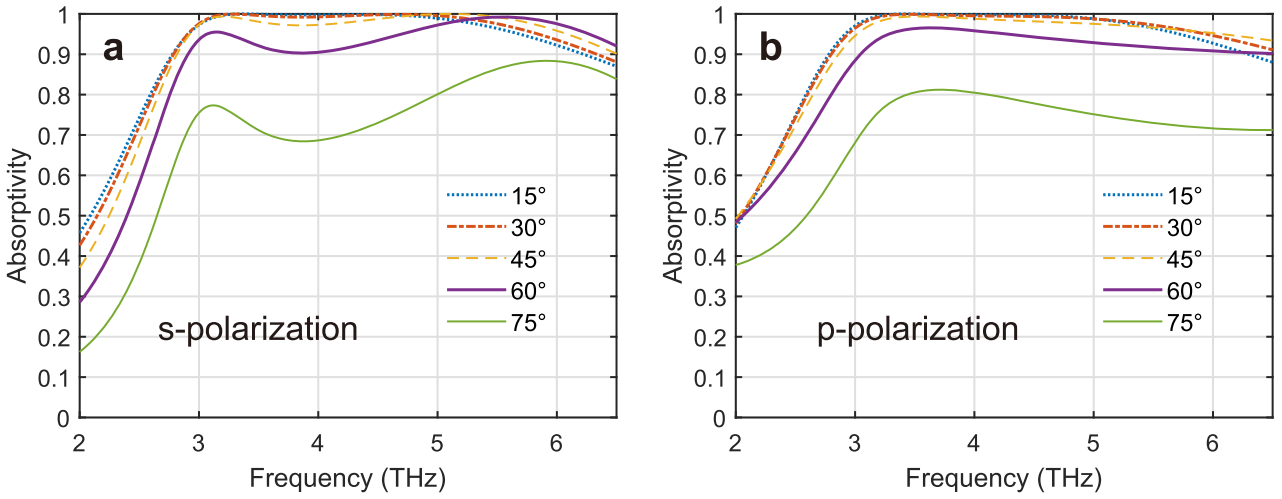

FIG. 4. Angular dependence of the broadband absorptivity spectra of the near-perfect absorber for s-polarization (a) and p-polarization (b), for angles of incidence equal to 15°, 30°, 45°, 60°, and 75°.

10 August 2023 06:08:03

© Author(s) 2023

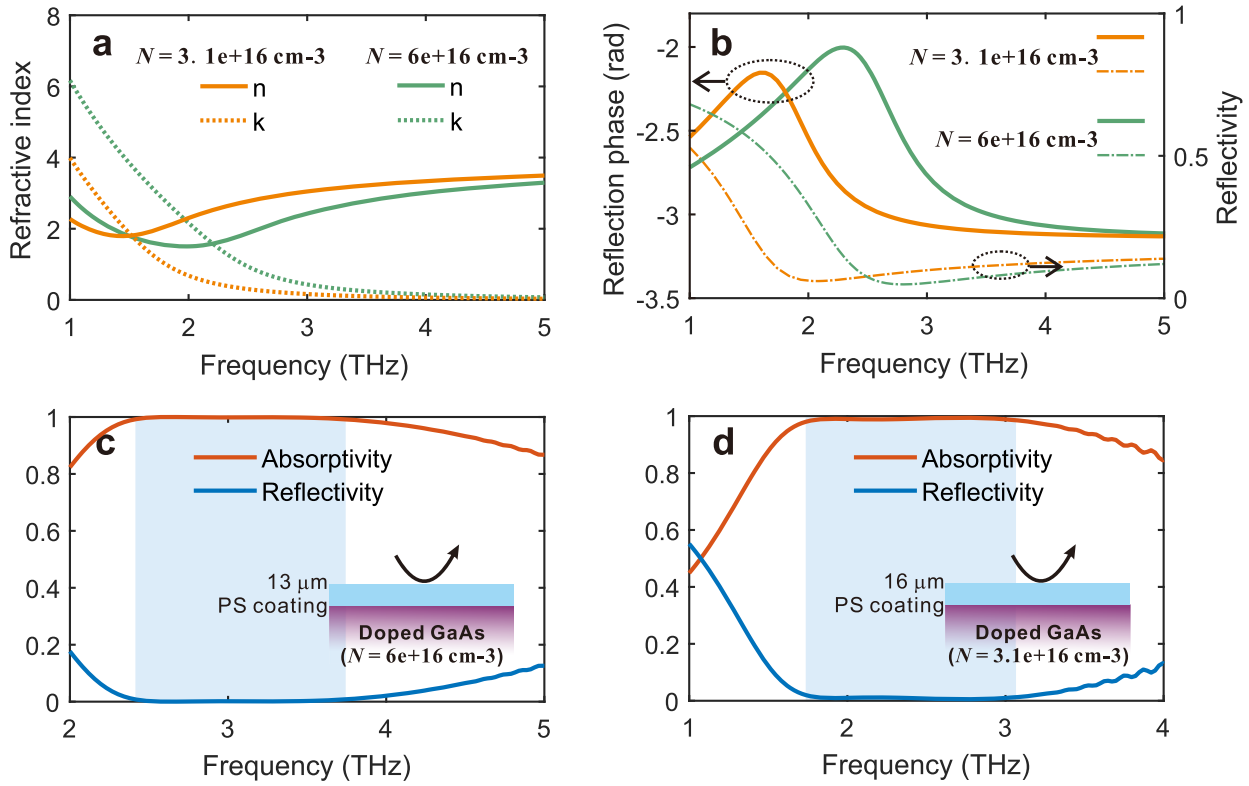

FIG. 5. (a) Complex refractive indices of the doped GaAs with carrier concentration of 3.1×10^{16} cm^{-3} and 6×10^{16} cm^{-3}. (b) The phase change and amplitude of the reflection from the air/doped-GaAs interface. (c) For $N = 6 \times 10^{16}$ cm^{-3}, a 13 μm-thick PS coating enables near-perfect absorption in the frequency range of 2.4–3.6 THz. (d) For $N = 3.1 \times 10^{16}$ cm^{-3}, a 16 μm-thick PS coating enables near-perfect absorption in 1.9–3 THz.

doped semiconductors can be greatly shifted by varying the doping concentration. Figure 5(a) shows the complex refraction indices of n-type doped GaAs with $N = 3.1 \times 10^{16}$ cm^{-3} ($\mu = 5500$ cm^2 V^{-1} s^{-1}) and $N = 6 \times 10^{16}$ cm^{-3} ($\mu = 5000$ cm^2 V^{-1} s^{-1}), respectively. The reflection phases and amplitudes from the PS/doped GaAs interfaces are also shown in Fig. 5(b). It can be observed that both the negative dispersion area of the reflection phase spectrum and the gentle dip in the reflection amplitude spectrum show an obvious red shift as the carrier concentration decreases. Additionally, it is worth noting that the morphology of the reflection amplitude and phase curves and the corresponding values are not significantly influenced by the carrier concentration. Thus, around the gentle dip in the spectrum, condition (i) can still be satisfied with the PS coating material, while condition (ii) requires adjusting the thickness of the PS coating film to follow the shifted frequency. In the case of doped GaAs with $N = 6 \times 10^{16}$ cm^{-3}, a 13 μm-thick PS coating can achieve broadband antireflection and near-perfect absorption in the frequency range of 2.4–3.6 THz [Fig. 5(c)]. For the case of doped GaAs with $N = 3.1 \times 10^{16}$ cm^{-3}, a 16 μm-thick PS coating can achieve near-perfect absorption in the range of 1.9–3 THz [Fig. 5(d)]. The observed ripples in the high-frequency region of the spectra are attributed to the resonant effects of the terahertz waves interacting with the substrate.

Similarly, a doped Si substrate with a coating of PE (Polyethylene)[41] can also enable broadband, near-complete antireflection in the terahertz frequencies. Figure 6(a) illustrates the schematic diagram of a bilayer structure of PE/doped Si. By using a bilayer structure composed of a 22 μm-thick PE coating and a 500 μm-thick doped Si substrate (carrier concentration $N = 4 \times 10^{16}$ cm^{-3}), a reflectivity of less than 5% is achieved over the frequency range from 1 to 1.75 THz, as shown in Fig. 6(b). According to conditions (i), the ideal refractive index value of the coating for a Si substrate with $N = 4 \times 10^{16}$ cm^{-3} can be derived to be 1.8. However, there is no common polymer with a refractive index of 1.8 in the lower terahertz frequency range. Therefore, PE is chosen as the coating material because its refractive index of 2 is very close to the ideal index value of 1.8. With PE coating, the reflection magnitude $|r|$ is only roughly approximated to $|\rho|$ in the 1–2 THz range, as shown in Fig. 6(c). This explains why the reflection cannot be completely eliminated by PE coating in Fig. 6(b). Regarding condition (ii), the round-trip phase Φ remains close to 0 in the 1–1.75 THz range, which is achieved through effective dispersion compensation between $\phi(\rho)$ and δ, as depicted in Fig. 6(d).

Table I summarizes the broadband absorbers designed in this work, demonstrating the general applicability of our proposed method for achieving near-perfect broadband absorption. The

10 August 2023 06:08:03

© Author(s) 2023

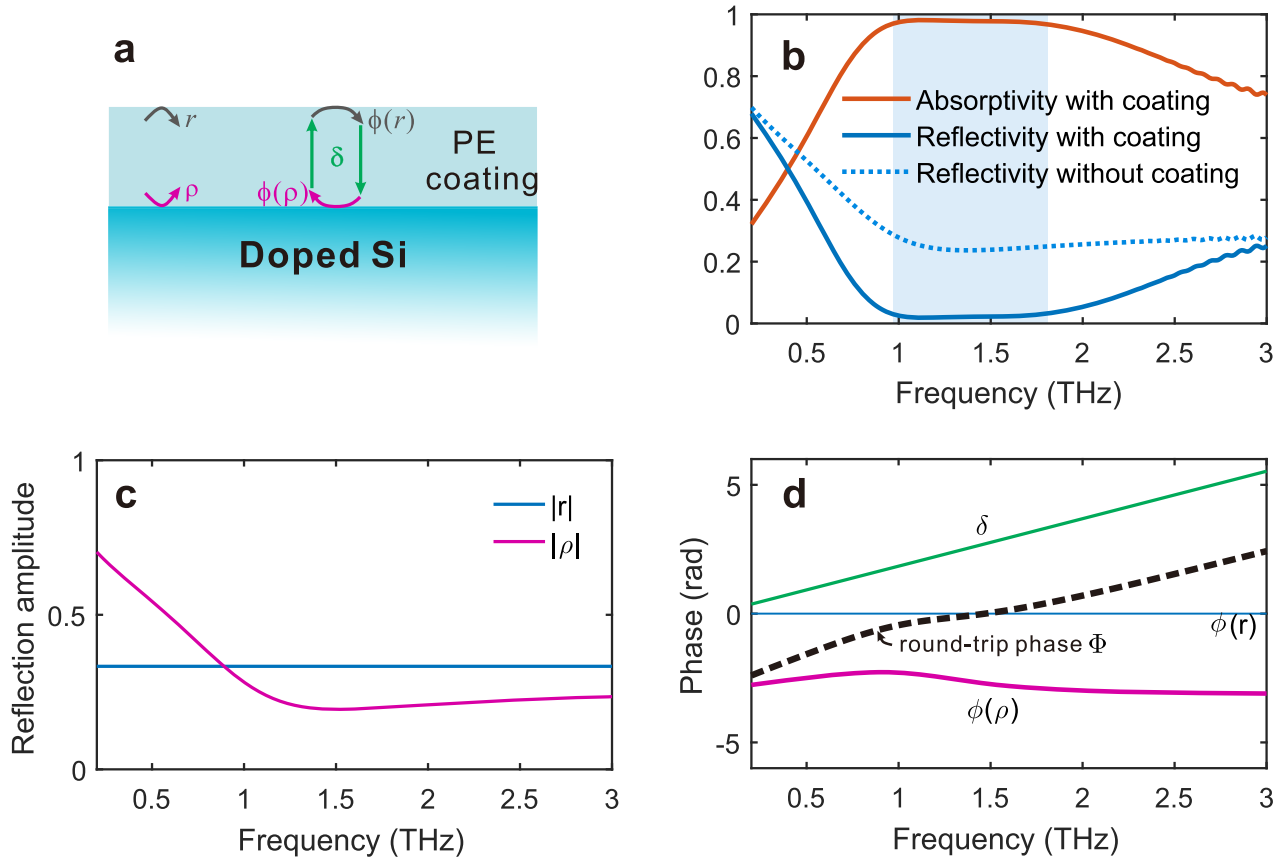

FIG. 6. (a) Schema of a doped Si substrate with PE coating. Here, the PE coating is 22 μm thick, and the carrier concentration of the *n*-type doped Si is 4×10^{16} cm^{-3}. (b) Absorptivity and reflectivity spectra of the doped Si with a PE coating layer, as well as the reflectivity spectra of the doped Si without the PE coating. (c) The spectra of reflection amplitudes $|r|$ and $|\rho|$. (d) The dispersion properties of phases $\phi(r)$, $\phi(\rho)$, δ, and Φ.

TABLE I. Comparison of the absorption bandwidths of the four broadband absorbers designed in this work.

Substrate	N (cm^{-3})	Coating	Thickness (μm)	Freq. (THz)	Abs. (%)
GaAs	10.3×10^{16}	PS	10	3.2–4.7	99
GaAs	6×10^{16}	PS	13	2.4–3.6	99
GaAs	3.1×10^{16}	PS	16	1.9–3	99
Si	4×10^{16}	PE	22	1–1.75	95

relative bandwidths of the four absorbers in the table are all above 38%, with the PE/doped-Si absorber achieving a relative bandwidth of 54%.

IV. CONCLUSION

In conclusion, we have proposed a simple and efficient method for achieving near-perfect absorption broadband. By applying a single-layer antireflection coating on a Drude-type substrate, we can achieve broadband antireflection through dispersion compensation, contrary to the well-known narrowband antireflection phenomenon. We have derived the conditions for the refractive indices of the coating and substrate that enable anomalous dispersion and phase shift upon reflection, facilitating dispersion compensation. Our simulation results demonstrate that the designed PS/doped-GaAs structure can achieve near-perfect absorption in the frequency range of 3.2–4.7 THz. Moreover, by adjusting the doping concentration in the semiconductor substrate and the thickness of the coating film, the absorption range can be tuned while maintaining broadband characteristics. This proposed strategy is simple and can be applied to other natural absorbers or artificial plasmonic structures.

ACKNOWLEDGMENTS

The support by the Natural Science Foundation of Anhui Province (Grant No. 808235830016), the Natural Science Foundation of Guangdong Province (Grant Nos. 2015A030311018 and 2017A030313035), and PolyU (G-UAGJ) is acknowledged.

10 August 2023 06:08:03

© Author(s) 2023

AUTHOR DECLARATIONS

Conflict of Interest

The authors have no conflicts to disclose.

Author Contributions

Fenghua Shi: Conceptualization (lead); Writing – original draft (lead). **Yihang Chen**: Supervision (equal); Writing – review & editing (equal). **Chi-Wah Leung**: Supervision (equal); Writing – review & editing (equal).

DATA AVAILABILITY

The data that support the findings of this study are available from the corresponding authors upon reasonable request.

REFERENCES

[1]Q. Xiao, T. U. Connell, J. J. Cadusch, A. Roberts, A. S. Chesman, and D. E. Gómez, "Hot-carrier organic synthesis via the near-perfect absorption of light," ACS Catal. **8**, 10331–10339 (2018).

[2]M. M. Hossain, B. Jia, and M. Gu, "A metamaterial emitter for highly efficient radiative cooling," Adv. Opt. Mater. **3**, 1047–1051 (2015).

[3]D. Liu, L. Wang, Q. Cui, and L. J. Guo, "Planar metasurfaces enable high-efficiency colored perovskite solar cells," Adv. Sci. **5**, 1800836 (2018).

[4]M. K. Akhlaghi, E. Schelew, and J. F. Young, "Waveguide integrated superconducting single-photon detectors implemented as near-perfect absorbers of coherent radiation," Nat. Commun. **6**, 8233 (2015).

[5]Y. Hu, M. Pantouvaki, J. Van Campenhout, S. Brems, I. Asselberghs, C. Huyghebaert, P. Absil, and D. Van Thourhout, "Broadband 10 Gb/s operation of graphene electro-absorption modulator on silicon," Laser Photonics Rev. **10**, 307–316 (2016).

[6]H. Sun, C. Gu, X. Chen, Z. Li, L. Liu, B. Xu, and Z. Zhou, "Broadband and broad-angle polarization-independent metasurface for radar cross section reduction," Sci. Rep. **7**, 40782 (2017).

[7]P. Baumeister, *Optical Coating Technology* (SPIE Press, 2004), Vol. 137.

[8]Z. Zhang, Y. Lv, X. Chen, Z. Wu, Y. He, L. Zhang, and Y. Zou, "Porous flower-like Ni/C composites derived from MOFs toward high-performance electromagnetic wave absorption," J. Magn. Magn. Mater. **487**, 165334 (2019).

[9]N. I. Landy, S. Sajuyigbe, J. J. Mock, D. R. Smith, and W. J. Padilla, "Perfect metamaterial absorber," Phys. Rev. Lett. **100**, 207402 (2008).

[10]S. Thongrattanasiri, F. H. Koppens, and F. J. G. García de Abajo, "Complete optical absorption in periodically patterned graphene," Phys. Rev. Lett. **108**, 047401 (2012).

[11]J. Grant, Y. Ma, S. Saha, A. Khalid, and D. R. Cumming, "Polarization insensitive, broadband terahertz metamaterial absorber," Opt. Lett. **36**, 3476–3478 (2011).

[12]S. Liu, H. Chen, and T. J. Cui, "A broadband terahertz absorber using multi-layer stacked bars," Appl. Phys. Lett. **106**, 151601 (2015).

[13]D.-H. Kim, D.-S. Kim, S. Hwang, and J.-H. Jang, "Surface relief structures for a flexible broadband terahertz absorber," Opt. Express **20**, 16815–16822 (2012).

[14]B.-X. Wang, C. Xu, G. Duan, W. Xu, and F. Pi, "Review of broadband metamaterial absorbers: From principles, design strategies, and tunable properties to functional applications," Adv. Funct. Mater. **33**, 2213818 (2023).

[15]B.-X. Wang, G. Duan, C. Xu, J. Jiang, W. Xu, and F. Pi, "Design of multiple-frequency-band terahertz metamaterial absorbers with adjustable absorption peaks using toothed resonator," Mater. Des. **225**, 111586 (2023).

[16]B.-X. Wang, C. Xu, H. Zhou, and G. Duan, "Realization of broadband terahertz metamaterial absorber using an anti-symmetric resonator consisting of two mutually perpendicular metallic strips," APL Mater. **10**, 050701 (2022).

[17]Y. Cui, K. H. Fung, J. Xu, H. Ma, Y. Jin, S. He, and N. X. Fang, "Ultrabroadband light absorption by a sawtooth anisotropic metamaterial slab," Nano Lett. **12**, 1443–1447 (2012).

[18]P. Yu, L. V. Besteiro, Y. Huang, J. Wu, L. Fu, H. H. Tan, C. Jagadish, G. P. Wiederrecht, A. O. Govorov, and Z. Wang, "Broadband metamaterial absorbers," Adv. Opt. Mater. **7**, 1800995 (2019).

[19]R.-H. Fan, B. Xiong, R.-W. Peng, and M. Wang, "Constructing metastructures with broadband electromagnetic functionality," Adv. Mater. **32**, e1904646 (2020).

[20]Z. Meng, C. Tian, C. Xu, J. Wang, S. Huang, X. Li, B. Yang, Q. Fan, and S. Qu, "Multi-spectral functional metasurface simultaneously with visible transparency, low infrared emissivity and wideband microwave absorption," Infrared Phys. Technol. **110**, 103469 (2020).

[21]D. Wu, Y. Liu, Z. Xu, Z. Yu, L. Yu, L. Chen, C. Liu, R. Li, R. Ma, J. Zhang, and H. Ye, "Numerical study of the wide-angle polarization-independent ultra-broadband efficient selective solar absorber in the entire solar spectrum," Sol. RRL **1**, 1700049 (2017).

[22]Y. Wu, Z. Qu, A. Osman, C. Wei, W. Cao, A. Tarazona, S. Z. Oo, H. M. Chong, O. L. Muskens, G. Z. Mashanovich, and M. Nedeljkovic, "Nanometallic antenna-assisted amorphous silicon waveguide integrated bolometer for mid-infrared," Opt. Lett. **46**, 677–680 (2021).

[23]X. Guo, X. Quan, Z. Li, Q. Li, B. Zhang, X. Zhang, and C. Song, "Broadband anti-reflection coatings fabricated by precise time-controlled and oblique-angle deposition methods," Coatings **11**, 492 (2021).

[24]Z. Liu, L. Guo, and Q. Zhang, "A simple and efficient method for designing broadband terahertz absorber based on singular graphene metasurface," Nanomaterials **9**, 1351 (2019).

[25]M. Huang, K. Wei, P. Wu, D. Xu, and Y. Xu, "Terahertz broadband absorber based on a combined circular disc structure," Micromachines **12**, 1290 (2021).

[26]Y. Huang, K. Kaj, C. Chen, Z. Yang, S. R. Ul Haque, Y. Zhang, X. Zhao, R. D. Averitt, and X. Zhang, "Broadband terahertz silicon membrane metasurface absorber," ACS Photonics **9**, 1150–1156 (2022).

[27]J. Ge, Y. Zhang, H. Li, H. Dong, and L. Zhang, "Ultra-broadband, tunable, and transparent microwave meta-absorber using ITO and water substrate," Adv. Opt. Mater. **11**, 2202873 (2023).

[28]Z. Zheng, Y. Zheng, Y. Luo, Z. Yi, J. Zhang, Z. Liu, W. Yang, Y. Yu, X. Wu, and P. Wu, "A switchable terahertz device combining ultra-wideband absorption and ultra-wideband complete reflection," Phys. Chem. Chem. Phys. **24**, 2527–2533 (2022).

[29]S.-C. Jiang, X. Xiong, Y.-S. Hu, Y.-H. Hu, G.-B. Ma, R.-W. Peng, C. Sun, and M. Wang, "Controlling the polarization state of light with a dispersion-free metastructure," Phys. Rev. X **4**, 021026 (2014).

[30]S. Wang, P. C. Wu, V.-C. Su, Y.-C. Lai, C. Hung Chu, J.-W. Chen, S.-H. Lu, J. Chen, B. Xu, C.-H. Kuan, T. Li, S. Zhu, and D. P. Tsai, "Broadband achromatic optical metasurface devices," Nat. Commun. **8**, 187 (2017).

[31]S.-C. Jiang, X. Xiong, Y.-S. Hu, S.-W. Jiang, Y.-H. Hu, D.-H. Xu, R.-W. Peng, and M. Wang, "High-efficiency generation of circularly polarized light via symmetry-induced anomalous reflection," Phys. Rev. B **91**, 125421 (2015).

[32]J. Kischkat, S. Peters, B. Gruska, M. Semtsiv, M. Chashnikova, M. Klinkmüller, O. Fedosenko, S. Machulik, A. Aleksandrova, G. Monastyrskyi, Y. Flores, and W. Ted Masselink, "Mid-infrared optical properties of thin films of aluminum oxide, titanium dioxide, silicon dioxide, aluminum nitride, and silicon nitride," Appl. Opt. **51**, 6789–6798 (2012).

[33]J. B. Pendry, A. Holden, D. Robbins, and W. Stewart, "Low frequency plasmons in thin-wire structures," J. Phys.: Condens. Matter **10**, 4785 (1998).

[34]J. B. Pendry, A. J. Holden, D. J. Robbins, and W. Stewart, "Magnetism from conductors and enhanced nonlinear phenomena," IEEE Trans. Microwave Theory Tech. **47**, 2075–2084 (1999).

[35]J. M. Ziman, *Principles of the Theory of Solids* (Cambridge University Press, 1972).

[36]Y.-S. Lee, *Principles of Terahertz Science and Technology* (Springer Science & Business Media, 2009), Vol. 170.

[37]P. Huggard, J. Cluff, G. Moore, C. Shaw, S. Andrews, S. Keiding, E. Linfield, and D. Ritchie, "Drude conductivity of highly doped GaAs at terahertz frequencies," J. Appl. Phys. **87**, 2382–2385 (2000).

10 August 2023 06:08:03

© Author(s) 2023

[38]S. Nashima, O. Morikawa, K. Takata, and M. Hangyo, "Measurement of optical properties of highly doped silicon by terahertz time domain reflection spectroscopy," Appl. Phys. Lett. **79**, 3923–3925 (2001).
[39]M. Born and E. Wolf, *Principles of Optics: Electromagnetic Theory of Propagation, Interference and Diffraction of Light* (Elsevier, 2013).
[40]C. C. Katsidis and D. I. Siapkas, "General transfer-matrix method for optical multilayer systems with coherent, partially coherent, and incoherent interference," Appl. Opt. **41**, 3978–3987 (2002).
[41]M. Naftaly and R. E. Miles, "Terahertz time-domain spectroscopy for material characterization," Proc. IEEE **95**, 1658–1665 (2007).
[42]R. Piesiewicz, C. Jansen, S. Wietzke, D. Mittleman, M. Koch, and T. Kürner, "Properties of building and plastic materials in the THz range," Int. J. Infrared, Millimeter, Waves **28**, 363–371 (2007).
[43]P. D. Cunningham, N. N. Valdes, F. A. Vallejo, L. M. Hayden, B. Polishak, X.-H. Zhou, J. Luo, A. K.-Y. Jen, J. C. Williams, and R. J. Twieg, "Broadband terahertz characterization of the refractive index and absorption of some important polymeric and organic electro-optic materials," J. Appl. Phys. **109**, 043505 (2011).
[44]M. A. Kats, R. Blanchard, P. Genevet, and F. Capasso, "Nanometre optical coatings based on strong interference effects in highly absorbing media," Nat. Mater. **12**, 20–24 (2013).

10 August 2023 06:08:03

© Author(s) 2023